Punjab University Journal of Mathematics (2024), 56(11), 723-752
https://doi.org/10.52280/pujm.2024.56(11)03

Bifurcation and Control of Rice Tungro Disease Spread in Plants Under Hypersensitive Response

Abdul Ghaffar
Department of Mathematics, Ghazi University D G Khan 32200, Pakistan
Email: abdulghaffar.jaffar@gmail.com
Khurram Faiz
Department of Mathematics, Ghazi University D G Khan 32200, Pakistan
Email: Corresponding author: khurram32103@gmail.com
Aqeel Ahmad
Department of Mathematics, Ghazi University D G Khan 32200, Pakistan
Mathematics Research Center, Near East University, Near East Boulevard, Nicosia North Cyprus, 99138
Email: aqeelahmad.740@gmail.com
Ghulam Mustafa
Department of Mathematics, The Islamia University Bahawalpur 63100, Pakistan
Email: ghulam.mustafa@iub.edu.pk
Muhammad Farman
Department of Mathematics, Near East University TRNC, Mersin 10, Nicosia 99138, Turkey
Research Center of Applied Mathematics, Khazar University, Baku, Azerbaijan
Email: farmanlink@gmail.com

Received:27 December, 2024 / Accepted:28 May, 2025 / Published online: 20 June, 2025

Abstract. The primary objective of this study is to investigate the spread of rice tungro disease within a community, with a particular focus on the role of predators in disease transmission. A mathematical model has been developed to examine the progression of rice tungro disease in a healthy environment, incorporating various control strategies such as the continuous removal of different categories of infected plants. To get proper numerical results, the rice tungro model is converted into a fractional rice model, and for fractional order, the fractal-fractional (FF) operator is used for continuous monitoring. The stability of the newly built model is checked by the quantitative and qualitative investigation. For a better understanding of the newly developed model, obtain the mathematical solution of the model with boundedness and uniqueness. The impact of different parameters on the spread of rice tungro disease is investigated. By using the Lipschitz condition and normed function, checking the spreads of rice tungro disease in all sub-compartmentss. Furthermore, the stability

of the model is examined by the Hyers-Ulam concept. The flip bifurcation is investigated for all compartments at equilibrium points, and a simulation for flip bifurcation is examined and see the effect of different variables on the spreading of disease across all compartments for flip bifurcation. Additionally, for numerical analysis of the fractional operator used the two-step Lagrange polynomial method was used for the generalized form with Mittag-Leffler kernel. Finally, numerical simulations are employed to demonstrate the effects of various factors on disease dynamics. Simulations have been conducted to observe the actual behavior and progression of rice tungro disease at various stages, using different parameter values in a healthy environment exhibiting a hypersensitive response (HR). This research contributes to a deeper understanding of disease transmission and supports the development of effective management strategies for plants based on validated findings.

AMS (MOS) Subject Classification Codes: 35B35; 26A16; 45M20; 37B25.
Key Words: Boundedness, Lipschitz Conditions, Positiveness, Rice Tungro, Stability Analysis.

1. Introduction

The Sustainable Development Goals (SDGs) include promoting sustainable agriculture and ensuring food security. One strategy to guarantee food security is to make staple foods like rice a staple meal made from rice plants available [19]. Measures must be taken to prevent diseases like tungro disease from spreading among rice plants to achieve this goal. The primary vector responsible for spreading tungro disease among rice plants is the green leafhopper. Two to three weeks after planting, plants will start to exhibit signs of tungro disease if infection happens at the nursery stage [13]. After rice is planted in the field, diseased and immature rice plants serve as the main source of inoculum. During a certain stage of growth, the number of infected plants can double. Immigrant insects were the source of the first infection peak, and infection with immigrant insect descendants was the reason for the second infection peak [18].

A key issue in global development is food security. Every individual, at all times, has physical and financial access to enough healthful food to suit their dietary needs and preferences for an active and healthy life, which is what is meant by [11]. The issue of food security is significantly influenced by the agricultural sector. A sustainable approach to agricultural growth and food security involves raising agricultural production [9]. However, a number of issues, particularly with regard to food crop commodities, contribute to a decline in both the amount and quality of agricultural production. Plant susceptibility to disease, pests, weather, and climate change is one of the primary determinants of it [7]. A mathematical model for plant diseases was created to give a thorough explanation of how to characterize, evaluate, and forecast plant disease outbreaks to create and evaluate crop protection control measures and strategies [12]. Plant epidemiology presents a number of significant challenges for human and animal disease models. Nevertheless, modeling plant diseases is complicated by several distinctive features of plant epidemiology [6].

Rice (Oryza sativa) is the most significant food crop in developing countries, since it is a staple diet for more than half of the world's population [10]. Since rice is a staple meal that many Asian communities depend on, rice harvests are currently the main source of concern. The prospective results of the rice varieties will not be achieved if the plants are infected with the Tungro virus [5]. There will be no repercussions even if the Tungro virus infection occurs during the early vegetative stage. The two related Tungro viral types that cause Tungro rice disease are the stem virus (Rice Tungro Bacilliform Virus: RTBV) and the spherical virus (Rice Tungro Spherical Virus: RTSV). Complex symptoms will be displayed by rice plants infected with two different strains of the Tungro virus. The symptoms are less severe if the plant is just infected with RTBV, but they are completely absent if it is only infected with RTSV. The green leafhopper Nephotettix virescens is the only semi-persistent carrier of both viruses. Rao discovered that as the vector population grew, so did the prevalence of RTV (Rice Tungro Virus) [15]. The Tungro virus must be managed in order to stop the spread of illness. Taking into account integrated pest and disease control techniques, effective cultural practices, and varietal resistance [1]. Insecticides are the most widely used strategy for managing the Tungro virus. Insecticide spraying aids in lowering the green leafhopper population, which delays the virus's transmission. Green leafhopper populations can be efficiently controlled using several standard insecticides.

Fractional calculus is used in many scientific fields, including physics and engineering. Fractional order models are preferable to ordinary integer order models because they can account for the genetic and memory components of systems [4]. Applications of fractional calculus can be found in many different and broad areas of science and engineering, including biological community models, optics, signal processing, fluid mechanics, electromagnetics, viscoelasticity, and electrochemistry. The primary objective of [8] was to examine the ocean system model by examining how predators are causing global climate change. A mathematical model has been developed using the hypothesis created for an ideal setting in order to examine the various incidences of Marburg virus disease following the implementation of control measures with implementation [14]. For different protection. Fractional calculus is used to create a mathematical model that includes control and asymptomatic variables to track the pace at which pine wilt changes. The model is reformulated as a fractional-order system using the Atangana–Baleanu–Caputo (ABC) operator, allowing for continuous monitoring [2]. According to [3], this method is crucial for comprehending the dynamics of illnesses that are common around the world. The optimal pH and temperature for this process were established, and the impact of the starting substrate concentration was evaluated [16]. Additionally, a fractional-order mathematical model including global properties of the Mittag-Leffler kernel characterized the results. In order to comprehend the entire dynamics of cholera and how the disease spreads across a population, mathematical formulas are a crucial tool [17].

To effectively control the rice tungro virus, particularly within populations of susceptible and infected individuals, this study introduces a novel approach that incorporates early detection and recovery-based control strategies. The main objective is to develop a new mathematical model that reflects the recovery impact of the disease in a healthy environment. Rice tungro is a highly destructive disease posing a serious threat to plant life. The study is structured to guide readers through its key components: Section 1 provides an introduction and historical background; Section 2 formulates the new recovery-based model

with proposed control measures; Section 3 analyzes the basic reproduction number along with the models equilibrium and endemic points; Section 4 investigates local stability using equilibrium analysis and the Jacobian matrix; Section 5 presents analytical results on positivity, boundedness, nonlocal operators, and the positive invariant region; Section 6 explores flip bifurcation through eigenvalue analysis and graphical simulations; Section 7 examines the effect of the global derivative using the Riemann-Stieltjes integral and norm; Section 8 develops numerical solutions using a fractional operator with a Mittag-Leffler kernel; Section 9 offers a detailed physical interpretation based on MATLAB simulations; and finally, Section 10 concludes with a summary of the main findings.

1.1. **Basic Results and Definitions. Definition. 1:** [8] Assume that $F(t)$ is fractal differentiable of order $\eta \in (0,1)$ and continuous on the interval (x,y). The **Fractal-Fractional derivative** in the sense of the Riemann–Liouville type with power-law kernel is defined as:

• For $0 \leq \eta, \beta \leq 1$, the kernel for a law of power is thus provided.

$$ {}_0^{FFP}D_t^{\eta,\beta}G(t) = \frac{1}{\Gamma(n+\eta)}\frac{d}{dt^\beta}\int_0^t (t-\beta)^{n-\eta-1}G(\beta)d\beta $$

where $\eta > n-1$, $\beta < n \in \mathbb{N}$. And

$$ \frac{DG(\beta)}{D\beta^\beta} = \lim_{t\to\beta}\frac{G(t)-G(\beta)}{t^\eta - \beta^\beta}. $$

• is stated using a kernel for exponential decay as follows:

$$ {}_0^{FFE}D_t^{\eta,\beta}G(t) = \frac{\mathcal{M}(\eta)}{\Gamma(n+\eta)}\frac{d}{dt^\beta}\int_0^t exp\left[-\frac{\eta}{1-\eta}(t-\beta)\right]G(\beta)d\beta $$

where $\eta > 0$, $\beta \leq n \in \mathbb{N}$, and $\mathcal{M}(0) = 1 = \mathcal{M}(1)$

• with an Mittag-Leffler kernel is expressed as:

$$ {}_0^{FFM}D_t^{\eta,\beta}G(t) = \frac{\mathcal{AB}(\eta)}{1-\eta}\frac{d}{dt^\beta}\int_0^t E_\eta\left[-\frac{\eta}{1-\eta}(t-\beta)^\eta\right]G(\beta)d\beta $$

where E_η and $0 < \eta, \beta \leq 1$ represent the Mittag-Leffler function, and $\mathcal{AB}(\eta) = 1-\eta+\frac{\eta}{\Gamma(\eta)}$ represents the normalization function.

Definition. 2: [8] The *Fractal-Fractional integral* of $G(t)$, with fractional order η and fractal order β, is continuous on the interval (x,y), provided that $0 \leq \eta, \beta \leq 1$ and $G(t)$ is continuous on (x,y).

• is provided using a power law kernel as follows:

$$ {}_0^{FFP}I^{\eta,\beta}G(t) = \frac{1}{\Gamma(\eta)}\int_0^t (t-\beta)^{\eta-1}\beta^{1-\beta}G(\beta)d\beta $$

• is written as follows for a kernel of exponential decay:

$$ {}_0^{FFE}I^{\eta,\beta}G(t) = \frac{\beta(1-\eta)t^{\beta-1}G(t)}{\mathcal{M}(\eta)} + \frac{\eta\beta}{\mathcal{M}(\eta)}\int_0^t \beta^{\eta-1}G(\beta)d\beta $$

• is expressed using a Mittag-Leffler kernel as

$$ {}_0^{FFM}I^{\eta,\beta}G(t) = \frac{\beta(1-\eta)t^{\rho-1}G(t)}{\mathcal{AB}(\eta)} + \frac{\eta\beta}{\mathcal{AB}(\eta)\Gamma(\eta)}\int_0^t (t-\beta)^{\eta-1}\beta^{\beta-1}G(\beta)d\beta. $$

2. Formulation of Rice Tungro disease

In order to maintain a healthy environment, this novel model for studying rice tungro disease introduces several metrics to assess various outcomes and enables early detection of infected plants, particularly those affected by stunted growth due to the disease. To the best of our knowledge, no previous study has proposed a model with the same structure as the one we present here, which incorporates multiple aspects of the disease's impact.

In this new framework, the plant population is categorized into four compartments. The generative-phase population of susceptible rice plants is denoted by S_g, and the generative-phase infected population by I_g. In the vegetative phase, healthy rice plants are represented by S_h, while infected rice plants are denoted by I_h. Additionally, two types of disease vectors are considered: susceptible vectors (S_v) and infected vectors (I_v). The model also accounts for carnivores, represented by P, which may influence the dynamics of disease spread by preying on vectors. The population of the model consists of different compartments, like as predators, rice plants at different stages, and vector beetles.

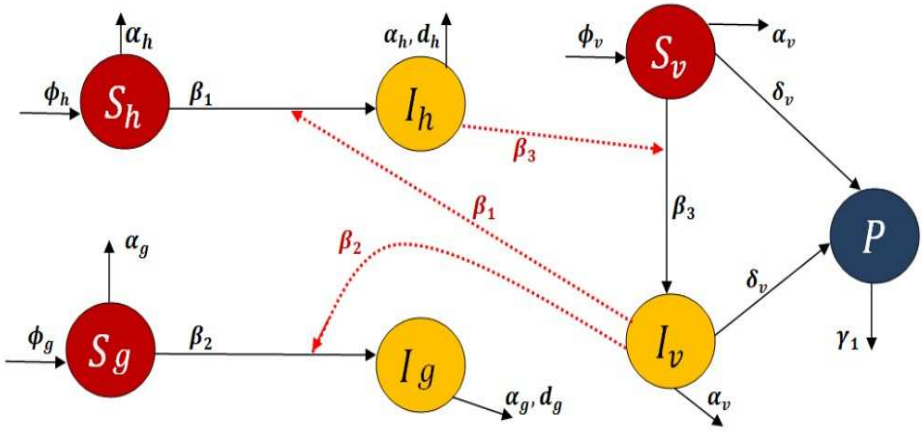

FIGURE 1. The newly created model is shown in the flow chart.

Different parameters are used with different characterization during the changing of healthy rice plants over the growing period. The birth rate of healthy plants is ϕ_h, the rate of transfer from susceptible to infected plants of the healthy category due to vector infection is β_1, and α_h is the rate of natural decay of healthy plants. The equation becomes:

$$DS_h = \phi_h - \beta_1 S_h I_v - \alpha_h S_h.$$

Rate of transfer from susceptible to infected plants of healthy category due to vector infected is β_1, d_h is the rate due to infection decay, and α_h is the rate of natural decay of healthy plants. The equation becomes:

$$DI_h = \beta_1 S_h I_v - (\alpha_h + d_h) I_h.$$

Different parameters are used with different characterization during the transition of healthy rice plants to the growing period. The birth rate of growing plants is ϕ_g, the rate of transfer from susceptible to infected plants of the growing category due to vector infection is β_2, and α_g is the rate of natural decay of growing plants. The equation becomes:

$$DS_g = \phi_g - \beta_2 S_g I_v - \alpha_g S_g.$$

Rate of transfer from susceptible to infected plants of growing category due to vector infection is β_2, d_g is the rate due to infection death, and α_g is the rate of natural decay of growing plants. The equation becomes:

$$DI_g = \beta_2 S_g I_v - (\alpha_g + d_g) I_g.$$

The birth rate of vectors is ϕ_v, the rate of transfer from susceptible to infected vectors due to the healthy infected class is β_3, δ_v transfer rate from susceptible vectors to predators, and α_v is the rate of natural decay of vectors. The equation becomes:

$$DS_v = \phi_v - \beta_3 S_v I_h - (\alpha_v + \delta_v) S_v.$$

The rate of transfer from susceptible to infected vectors due to the healthy infected class is β_3, the δ_v transfer rate from susceptible vectors to predators, and α_v is the rate of natural decay of vectors. The equation becomes:

$$DI_v = \beta_3 S_v I_h - (\alpha_v + \delta_v) I_v.$$

The δ_v transfer rate from both vectors, susceptible and infected, to predators and γ_1 is the rate of natural decay of predators. The equation becomes:

$$\frac{dP}{dt} = \delta_v (S_v + I_v) - \gamma_1 P.$$

This equation shows how the populations of disease-carrying vectors and predators change over time.

Consequently, the differential equations system has been represented using a flow chart, along with our proposed hypothesis, illustrating an epidemic model with nonlinear incidence and a host vector.

$$\begin{aligned}
DS_h =& \phi_h - \beta_1 S_h I_v - \alpha_h S_h; \\
DI_h =& \beta_1 S_h I_v - (\alpha_h + d_h) I_h; \\
DS_g =& \phi_g - \beta_2 S_g I_v - \alpha_g S_g; \\
DI_g =& \beta_2 S_g I_v - (\alpha_g + d_g) I_g; \\
DS_v =& \phi_v - \beta_3 S_v I_h - (\alpha_v + \delta_v) S_v; \\
DI_v =& \beta_3 S_v I_h - (\alpha_v + \delta_v) I_v; \\
DP =& \delta_v (S_v + I_v) - \gamma_1 P.
\end{aligned} \tag{2. 1}$$

with the following initial conditions: $S_h(0) = S_h^0$, $I_h(0) = I_h^0$, $S_g(0) = S_g^0$, $I_g(0) = I_g^0$, $S_v(0) = S_v^0$, $I_v(0) = I_v^0$, $P(0) = P^0$.

Using the notion of a fractal fractional derivative on the differential equation system above, we now obtain

$$
\begin{aligned}
{}_0^{FFM}D_t^{\eta,\beta}S_h &= \phi_h - \beta_1 S_h I_v - \alpha_h S_h;\\
{}_0^{FFM}D_t^{\eta,\beta}I_h &= \beta_1 S_h I_v - (\alpha_h + d_h) I_h;\\
{}_0^{FFM}D_t^{\eta,\beta}S_g &= \phi_g - \beta_2 S_g I_v - \alpha_g S_g;\\
{}_0^{FFM}D_t^{\eta,\beta}I_g &= \beta_2 S_g I_v - (\alpha_g + d_g) I_g;\\
{}_0^{FFM}D_t^{\eta,\beta}S_v &= \phi_v - \beta_3 S_v I_h - (\alpha_v + \delta_v) S_v;\\
{}_0^{FFM}D_t^{\eta,\beta}I_v &= \beta_3 S_v I_h - (\alpha_v + \delta_v) I_v;\\
{}_0^{FFM}D_t^{\eta,\beta}P &= \delta_v (S_v + I_v) - \gamma_1 P.
\end{aligned}
\tag{2. 2}
$$

The fractal fractional operator of Mittag-Leffler in this case is ${}_0^{FFM}D_t^{\eta,\beta}$, where $0 < \eta \leq 1$ and $0 < \beta \leq 1$. The system under description is associated with the initial conditions $S_h(0) = S_h^0$, $I_h(0) = I_h^0$, $S_g(0) = S_g^0$, $I_g(0) = I_g^0$, $S_v(0) = S_v^0$, $I_v(0) = I_v^0$, $P(0) = P^0$.

3. Analysis of Model

3.1. **Positivity and Bounded-ness.**

Theorem 3.2. *Assume that initial state values be* $(S_h(0), I_h(0), S_g(0), I_g(0), S_v(0), I_v(0), P(0) > 0)$. *Then, the solution set* $\Psi = \{S_h, I_h, S_g, I_g, S_v, I_v, P\} \in \mathbb{R}_7^+$ *of the rice tungro disease model (2. 2) are positive for all* $t > 0$. *Furthermore*

$$\lim_{t\to\infty} \sup N_h \leq \frac{\phi_h}{\alpha_h}, \lim_{t\to\infty} \sup N_g \leq \frac{\phi_g}{\alpha_g}, \lim_{t\to\infty} \sup N_v \leq \frac{\phi_v}{\alpha_v + \delta_v}, \lim_{t\to\infty} \sup P \leq \frac{\delta_v N_v}{\gamma_1}$$

with $N_h = S_h + I_h$, $N_g = S_g + I_g$, $N_v = S_v + I_v$.

Proof: Let $t_1 = \sup\{t > 0 : S_h(0) > 0, I_h(0) > 0, S_g(0) > 0, I_g(0) > 0, S_v(0) > 0, I_v(0) > 0, P(0) > 0\} \in [0, T]$. If every initial value is 0, we have nothing to prove. Thus, if we allow the initial data to be more than zero, $T_1 > 0$. The initial dynamical equation of the model (2. 2) states that

$$DS_h = \phi_h - \beta_1 S_h I_v - \alpha_h S_h.$$

Solving for $S_h(t_1)$ from the above equation using the integrating factor technique yields

$$\frac{d}{dt}\{[(\beta_1 I_v + \alpha_h)t] S_h\} = \phi_h \exp[(\beta_1 I_v + \alpha_h)t].$$

So

$$S_h(t_1)\exp[(\beta_1 I_v + \alpha_h)t_1] - S_h(0) = \int_0^{t_1} \phi_h \exp[(\beta_1 I_v + \alpha_h)x]dx.$$

Which leads to

$$S_h(t_1) = S_h(0)\exp[-(\beta_1 I_v + \alpha_h)t_1] + \exp[-(\beta_1 I_v + \alpha_h)t_1] \int_0^{t_1} \phi_h \exp[(\beta_1 I_v + \alpha_h)x]dx.$$

Also from the third equation of model (2. 2), $S_g(t_1)$can be obtained. Thus

$$S_g(t_1) = S_g(0)\exp[-(\beta_2 I_v + \alpha_g)t_1] + \exp[-(\beta_2 I_v + \alpha_g)t_1] \int_0^{t_1} \phi_g \exp[(\beta_2 I_v + \alpha_g)x]dx.$$

It is also possible to extract $S_v(t_1)$ from the fifth equation of the model (2. 2). Thus

$$\begin{aligned} S_v(t_1) &= S_g(0)\exp[-(\beta_3 I_h+\alpha_v+\delta_v)t_1]+\exp[-(\beta_3 I_h+\alpha_v+\delta_v)t_1] \\ &\int_0^{t_1}\phi_v\exp[(\beta_3 I_h+\alpha_v+\delta_v)x]dx. \end{aligned}$$

Also from the last equation of model (2. 2), $P(t_1)$can be obtained. Thus

$$P(t_1)=P(0)\exp[-(\gamma_1)t_1]+\exp[-(\gamma_1)t_1]\int_0^{t_1}(\delta_v)N_v\exp[(\gamma_1)x]dx.$$

Thus, for every $t>0$, $I_h>0$, $I_g>0$, and $I_v>0$, it can be shown that. We now prove that the total population of the climate change model compartments remains bounded as time progresses, thereby completing the second part of Theorem 3.2. $0<S_h+I_h\leq N_h$, $0<S_g+I_g\leq N_g$, $0<S_v+I_v\leq N_v$, and $0<P(t)\leq P(t)$, assuming the following. The entire population is given by the model (2. 2) as

$$\frac{dN_h}{dt} = \phi_h-\alpha_h(S_h+I_h)-d_hI_h<\phi_h-\alpha_h(S_h+I_h), \tag{3. 3}$$

$$\frac{dN_g}{dt} = \phi_g-\alpha_g(S_g+I_g)-d_gI_g<\phi_g-\alpha_g(S_g+I_g), \tag{3. 4}$$

$$\frac{dN_h}{dt} = \phi_v-(\alpha_v+\delta_v)(S_v+I_v), \tag{3. 5}$$

$$\frac{dP}{dt} = \delta_vN_v-\gamma_1P. \tag{3. 6}$$

Thus,

$$\begin{aligned} \phi_h-\alpha_hN_h &\leq \frac{dN_h}{dt}\leq\phi_h-\alpha_hN_h, \\ \phi_g-\alpha_gN_g &\leq \frac{dN_g}{dt}\leq\phi_g-\alpha_gN_g, \\ \phi_v-(\alpha_v+\delta_v)N_v &\leq \frac{dN_v}{dt}\leq\phi_v-(\alpha_v+\delta_v)N_v, \\ \delta_vN_v-\gamma_1P &\leq \frac{dP}{dt}\leq\delta_vN_v-\gamma_1P. \end{aligned}$$

Hence,

$$\begin{aligned} \frac{\phi_h}{\alpha_h} &\leq \liminf_{t\to\infty}N_h\leq\limsup_{t\to\infty}N_h\leq\frac{\phi_h}{\alpha_h}, \\ \frac{\phi_g}{\alpha_g} &\leq \liminf_{t\to\infty}N_g\leq\limsup_{t\to\infty}N_g\leq\frac{\phi_g}{\alpha_g}, \\ \frac{\phi_v}{\alpha_v+\delta_v} &\leq \liminf_{t\to\infty}N_v\leq\limsup_{t\to\infty}N_v\leq\frac{\phi_h}{\alpha_v+\delta_v}, \\ \frac{N_v\delta_v}{\gamma_1} &\leq \liminf_{t\to\infty}P\leq\limsup_{t\to\infty}P\leq\frac{N_v\delta_v}{\gamma_1}, \end{aligned}$$

complete the proof.

3.3. **Invariant regions.** By considering the epidemiological feasible region $\mathcal{P} \subset \mathbb{R}^7_+$, defined as below, we aim to verify that the trajectories of the rice tungro model (2. 2) remain within a realistic bounded domain for all $t > 0$.

$$\Psi = \Psi_h + \Psi_g + \Psi_v + \Psi_P \subset \mathbb{R}^2_+ \times \mathbb{R}^2_+ \times \mathbb{R}^2_+ \times \mathbb{R}^1_+$$

where

$$\Psi = \left\{ (S_h, I_h, S_g, I_g, S_v, I_v, P) \in \mathbb{R}^+_7 : N_h \leq \frac{\phi_h}{\alpha_h}, N_g \leq \frac{\phi_g}{\alpha_g}, N_v \leq \frac{\phi_v}{\alpha_v + \delta_v}, P \leq \frac{\delta_v N_v}{\gamma_1} \right\}.$$

We now review the following Eqs to prove that $\mathbb{R}^+_7$ is positively invariant. Here, it should be mentioned that if $0 < I_h \leq N_h$, $0 < I_g \leq N_g$, and $0 < I_v \leq N_v$, then it follows that (3. 3), (3. 4), (3. 5), and (3. 6)

$$\begin{aligned}
\frac{dN_h}{dt} &\leq \phi_h - \alpha_h N_h, \\
\frac{dN_g}{dt} &\leq \phi_g - \alpha_g N_g, \\
\frac{dN_h}{dt} &\leq \phi_v - (\alpha_v + \delta_v) N_v \\
\frac{dP}{dt} &\leq \delta_v N_v - \gamma_1 P.
\end{aligned}$$

The following is established when the aforementioned inequalities are solved. $N_h(t) \leq N_h(0)e^{-\alpha_h t} + \frac{\phi_h}{\alpha_h}(1 - e^{-\alpha_h t})$, $N_g(t) \leq N_g(0)e^{-\alpha_g t} + \frac{\phi_g}{\alpha_g}(1 - e^{-\alpha_g t})$, $N_v(t) \leq N_v(0)$ $e^{-\alpha_v + \delta_v t} + \frac{\phi_v}{\alpha_v + \delta_v}\left(1 - e^{-\alpha_v + \delta_v t}\right)$ and $P(t) \leq P(0)e^{-\gamma_1 t} + \frac{\delta_v N_v}{\gamma_1}(1 - e^{-\gamma_1 t})$. Specifically $N_h \leq \frac{\phi_h}{\alpha_h}$, $N_g \leq \frac{\phi_g}{\alpha_g}$, $N_v \leq \frac{\phi_v}{\alpha_v + \delta_v}$, $P \leq \frac{\delta_v N_v}{\gamma_1}$ as $t \to \infty$. As a result, the region Ψ is positively invariant. Therefore, it is sufficient to conclude that all solutions of the rice tungro disease model, starting from initial conditions within the feasible region Ψ, remain in this region for all future times. This confirms that the proposed model is epidemiologically meaningful and mathematically well-posed.

3.4. **Analysis of Existence for solution.** We aim to determine the existence of solutions for the fractal-fractional model of rice tungro disease given by equation (2. 2) using the fixed-point theorem. Accordingly, we have:

$$\begin{aligned}
S_h(t) - S_h(0) &= \frac{\beta\, \eta}{\Gamma(\eta)\, KM(\eta)} \int_0^t p^{\beta-1}(t-p)^{\eta-1}(\phi_h - \beta_1 S_h I_v - \alpha_h S_h)dp \\
&+ \frac{\beta(1-\eta)t^{\beta-1}}{KM(\eta)}(\phi_h - \beta_1 S_h I_v - \alpha_h S_h),
\end{aligned}$$

Let us now define a set of constants r_i, where $i \in \mathbb{N}^7_1$, along with

$$\begin{aligned}
\mathbf{C}_1(t,S_h) &= \phi_h - \beta_1 S_h I_v - \alpha_h S_h, \quad \mathbf{C}_2(t,I_h) = \beta_1 S_h I_v - (\alpha_h + d_h) I_h;\\
\mathbf{C}_3(t,S_g) &= \phi_g - \beta_2 S_g I_v - \alpha_g S_g, \quad \mathbf{C}_4(t,I_g) = \beta_2 S_g I_v - (\alpha_g + d_g) I_g;\\
\mathbf{C}_5(t,S_v) &= \phi_v - \beta_3 S_v I_h - (\alpha_v + \delta_v) S_v, \quad \mathbf{C}_6(t,I_v) = \beta_3 S_v I_h - (\alpha_v + \delta_v) I_v;\\
\mathbf{C}_7(t,P) &= \delta_v (S_v + I_v) - \gamma_1 P.
\end{aligned}$$

† To support our findings, the following assumptions are considered: the functions S_h, I_h, S_g, I_g, S_v, I_v, P, and $S_h^\star$ are continuous. Furthermore, the functions $I_h^\star$, $S_g^\star$, $I_g^\star$, $S_v^\star$, $I_v^\star$, and $P^\star$ belong to the space $\mathbf{L}[0,1]$. It is also assumed that there exist constants k_1, k_2, and k_3 such that $\|I_h\| \leq k_1$, $\|I_g\| \leq k_2$, and $\|I_v\| \leq k_3$.

Theorem 3.5. *Assuming that condition* (†) *holds, the kernels* $\mathbf{C}_i$*, for* $i = 1, 2, \ldots, 7$*, satisfy the Lipschitz condition and fulfill the inequality* $j_i < 1$ *for all* $i \in \mathbb{N}_1^7$.

Proof: The proof is omitted as it follows similarly to the approach in [3].

Equation (3. 7) is rewritten using the kernels, with the initial conditions $S_h(0) = 0$, $I_h(0) = 0$, $S_g(0) = 0$, $I_g(0) = 0$, $S_v(0) = 0$, $I_v(0) = 0$, and $P(0) = 0$, which leads to:

$$\begin{aligned}
S_h(t) &= \frac{\beta\,\eta}{\Gamma(\eta)\,KM(\eta)} \int_0^t p^{\beta-1}(t-p)^{1-\eta} \mathbf{C}_1(p, S_h(p))dp\\
&+ \frac{\beta(1-\eta)\,t^{\beta-1}}{KM(\eta)} \mathbf{C}_1(t, S_h(t)), \qquad (3.\ 7)\\
I_h(t) &= \frac{\beta\,\eta}{\Gamma(\eta)\,KM(\eta)} \int_0^t p^{\beta-1}(t-p)^{1-\eta} \mathbf{C}_2(p, I_h(p))dp + \frac{\beta(1-\eta)\,t^{\beta-1}}{KM(\eta)} \mathbf{C}_2(t, I_h(t)),
\end{aligned}$$

Now, we state the following formulas recursively.

$$\begin{aligned}
S_{h_n}(t) &= \frac{\beta\,\eta}{\Gamma(\eta)\,KM(\eta)} \int_0^t p^{\beta-1}(t-p)^{1-\eta} \mathbf{C}_1(p, S_{h_{n-1}}(p))dp + \frac{\beta(1-\eta)\,t^{\beta-1}}{KM(\eta)} \mathbf{C}_1(t, S_{h_{n-1}}(t)),\\
I_{h_n}(t) &= \frac{\beta\,\eta}{\Gamma(\eta)\,KM(\eta)} \int_0^t p^{\beta-1}(t-p)^{1-\eta} \mathbf{C}_2(p, I_{h_{n-1}}(p))dp + \frac{\beta(1-\eta)\,t^{\beta-1}}{KM(\eta)} \mathbf{C}_2(t, I_{h_{n-1}}(t)),
\end{aligned}$$

Further, let us consider the following differences, $\mathbf{G}^*$:

$$\begin{aligned}
\mathbf{G}^*(S_{h_{n+1}}(t)) &= S_{h_{n+1}} - S_{h_n} = \frac{\beta\,\eta}{\Gamma(\eta)\,KM(\eta)} \int_0^t p^{\beta-1}(t-p)^{1-\eta} \mathbf{C}_1(p, S_{h_n}(p))dp\\
&+ \frac{\beta(1-\eta)\,t^{\beta-1}}{KM(\eta)} \mathbf{C}_1(t, S_{h_n}(t)) - \Bigg(\frac{\beta\,\eta}{\Gamma(\eta)\,KM(\eta)} \int_0^t p^{\beta-1}(t-p)^{1-\eta}\\
&\mathbf{C}_1(p, S_{h_{n-1}}(p))dp + \frac{\beta(1-\eta)\,t^{\beta-1}}{KM(\eta)} \mathbf{C}_1(t, S_{h_{n-1}}(t)) \Bigg),
\end{aligned}$$

Imposing norm on $\mathbf{G}^*$, we get

$$\begin{aligned}\|\mathbf{G}^*(S_{h_{n+1}}(t))\| &= \|S_{h_{n+1}} - S_{h_n}\| = \left\| \frac{\beta\,\eta}{\Gamma(\eta)\,KM(\eta)} \int_0^t p^{\beta-1}(t-p)^{1-\eta}\mathbf{C}_1(p, S_{h_n}(p))dp \right. \\ &+ \frac{\beta(1-\eta)\,t^{\beta-1}}{KM(\eta)}\mathbf{C}_1(t, S_{h_n}(t)) - \left(\frac{\beta\,\eta}{\Gamma(\eta)\,KM(\eta)} \int_0^t p^{\beta-1}(t-p)^{1-\eta} \right. \\ &\left. \left. \mathbf{C}_1(p, S_{h_{n-1}}(p))dp + \frac{\beta(1-\eta)\,t^{\beta-1}}{KM(\eta)}\mathbf{C}_1(t, S_{h_{n-1}}(t)) \right) \right\|, \\ &= \frac{\beta\,\eta}{\Gamma(\eta)\,KM(\eta)} \int_0^t p^{\beta-1}(t-p)^{1-\eta}\|\mathbf{C}_1(p, S_{h_n}(p))dp - \mathbf{C}_1(p, S_{h_{n-1}}(p))dp\| + \\ &\frac{\beta(1-\eta)\,t^{\beta-1}}{KM(\eta)}\|\mathbf{C}_1(t, S_{h_n}(t)) - \mathbf{C}_1(t, S_{h_{n-1}}(t))\|.\end{aligned}$$

Similarly, for the remaining equations in (2. 2), we proceed in the same manner as demonstrated for the equation of $S_h(t)$.

Theorem 3.6. *The following conditions must be met for the fractal-fractional rice tungro illness model to have a solution:*

$$l_i = \max\{j_1, j_2, j_3, j_4, j_5, j_6, j_7\} < 1.$$

Proof: We now define the following functions:

$$\begin{cases} \mathbf{K}_1(n)t = S_{h_{n+1}} - S_{h_n}, & \mathbf{K}_2(n)t = I_{h_{n+1}} - I_{h_n}, \\ \mathbf{K}_3(n)t = S_{g_{n+1}} - S_{g_n}, & \mathbf{K}_4(n)t = I_{g_{n+1}} - I_{g_n}, \\ \mathbf{K}_5(n)t = S_{v_{n+1}} - S_{v_n}, & \mathbf{K}_6(n)t = I_{v_{n+1}} - I_{v_n}, \\ \mathbf{K}_7(n)t = P_{n+1} - P_n, & \end{cases} \tag{3. 8}$$

Imposing norms on (3. 8), results in

$$\begin{aligned}\|\mathbf{K}_1(n)t\| &= \|S_{h_{n+1}} - S_h\| = \left\| \frac{\beta\,\eta}{\Gamma(\eta)\,KM(\eta)} \int_0^t p^{\beta-1}(t-p)^{1-\eta}\mathbf{C}_1(p, S_{h_n}(p))dp \right. \\ &+ \frac{\beta(1-\eta)\,t^{\beta-1}}{KM(\eta)}\mathbf{C}_1(t, S_{h_n}(t)) - \left(\frac{\beta\,\eta}{\Gamma(\eta)\,KM(\eta)} \int_0^t p^{\beta-1}(t-p)^{1-\eta} \right. \\ &\left. \left. \mathbf{C}_1(p, S_h(p))dp + \frac{\beta(1-\eta)\,t^{\beta-1}}{KM(\eta)}\mathbf{C}_1(t, S_h(t)) \right) \right\|, \\ &= \frac{\beta\,\eta}{\Gamma(\eta)\,KM(\eta)} \int_0^t p^{\beta-1}(t-p)^{1-\eta}\|\mathbf{C}_1(p, S_{h_n}(p))dp - \mathbf{C}_1(p, S_h(p))dp\| + \\ &\frac{\beta(1-\eta)\,t^{\beta-1}}{KM(\eta)}\|\mathbf{C}_1(t, S_{h_n}(t)) - \mathbf{C}_1(t, S_h(t))\|\end{aligned}$$

$$\begin{aligned}\|\mathbf{K}_1(n)t\| &\leq \left(\frac{\beta\,\eta}{\Gamma(\eta)\,KM(\eta)}\int_0^t p^{\beta-1}(t-p)^{1-\eta}+\frac{\beta(1-\eta)\,t^{\beta-1}}{KM(\eta)}\right)j_1\|S_{h_n}(t)-S_h(t)\|\\ &\leq \left(\frac{\eta\,\beta\Gamma(\beta)}{KM(\eta)\,\Gamma(\eta+\beta)}+\frac{\beta(1-\eta)}{KM(\eta)}\right)j_1\|S_{h_n}(t)-S_h(t)\|\\ &\leq \left(\frac{\eta\,\beta\Gamma(\beta)}{KM(\eta)\,\Gamma(\eta+\beta)}+\frac{\beta(1-\eta)}{KM(\eta)}\right)^n l^n\|S_{h_1}(t)-S_h(t)\|\end{aligned}$$

Where $l<1$, and as $n\to\infty$, it follows that $S_{h_n}\to S_h$. By applying the following integral formula:

$$A(a,b)=(v-a)^{-a+b+1}\int_u^v (x-u)^{a-1}(v-x)^{b-1}\,dx,$$

and considering $t\in[0,T]$, we have $t^{-1-\eta+\beta}\leq 1$ and $t^{\beta}\leq 1$. Similarly, for the remaining equations in (2. 2), we proceed as done for the equation of $S_h(t)$. This concludes the proof.

3.7. **Uniqueness of model's solution.**

Theorem 3.8. *If the following inequalities hold, then the fractal-fractional rice tungro disease model given by (2. 2) admits a unique solution:*

$$\left(\frac{\eta\,\beta\Gamma(\beta)}{KM(\eta)\,\Gamma(\eta+\beta)}+\frac{\beta(1-\eta)}{KM(\eta)}\right)j_i\leq 1\quad i\in\mathbb{N}_1^7.$$

Proof: Examine the paradox that, for the fractal-fractional rice tungro illness model (2. 2), there is an alternative solution such that

$$\begin{aligned}S_h^*(t) &= \frac{\beta\,\eta}{\Gamma(\eta)\,KM(\eta)}\int_0^t p^{\beta-1}(t-p)^{1-\eta}\mathbf{C}_1(p,S_h^*(p))dp+\frac{\beta(1-\eta)\,t^{\beta-1}}{KM(\eta)}\mathbf{C}_1(t,S_h^*(t)),\\ I_h^*(t) &= \frac{\beta\,\eta}{\Gamma(\eta)\,KM(\eta)}\int_0^t p^{\beta-1}(t-p)^{1-\eta}\mathbf{C}_2(p,I_h^*(p))dp+\frac{\beta(1-\eta)\,t^{\beta-1}}{KM(\eta)}\mathbf{C}_2(t,I_h^*(t)),\end{aligned}$$

Taking the variation in the norms of S_h, S_h^*, we get

$$\begin{aligned}\|S_h(t)-S_h^*(t)\| &= \Bigg\|\frac{\beta\,\eta}{\Gamma(\eta)\,KM(\eta)}\int_0^t p^{\beta-1}(t-p)^{1-\eta}\mathbf{C}_1(p,S_h(p))dp+\frac{\beta(1-\eta)\,t^{\beta-1}}{KM(\eta)}\mathbf{C}_1(t,S_h(t))-\\ &\quad\left(\frac{\beta\,\eta}{\Gamma(\eta)\,KM(\eta)}\int_0^t p^{\beta-1}(t-p)^{1-\eta}\mathbf{C}_1(p,S_h^*(p))dp+\frac{\beta(1-\eta)\,t^{\beta-1}}{KM(\eta)}\mathbf{C}_1(t,S_h^*(t))\right)\Bigg\|,\\ &= \frac{\beta\,\eta}{\Gamma(\eta)\,KM(\eta)}\int_0^t p^{\beta-1}(t-p)^{1-\eta}\|\mathbf{C}_1(p,S_h(p))-\mathbf{C}_1(p,S_h^*(p))\|dp\\ &+ \frac{\beta(1-\eta)\,t^{\beta-1}}{KM(\eta)}\|\mathbf{C}_1(t,S_h(t))-\mathbf{C}_1(t,S_h^*(t))\|\\ &\leq \left(\frac{\beta\,\eta}{\Gamma(\eta)\,KM(\eta)}\int_0^t p^{\beta-1}(t-p)^{1-\eta}+\frac{\beta(1-\eta)\,t^{\beta-1}}{KM(\eta)}\right)j_1\|S_h(t)-S_h^*(t)\|\\ &\quad\times\left[1-\left(\frac{\eta\,\beta\Gamma(\beta)}{KM(\eta)\,\Gamma(\eta+\beta)}+\frac{\beta(1-\eta)}{KM(\eta)}\right)\right]\|S_h(t)-S_h^*(t)\|<0.\end{aligned}$$

Above inequality is true if $\|S_h(t) - S_h^*(t)\| = 0$, thus $S_h^*(t) = S_h(t)$. Similarly, for the remaining equations in (2. 2), we follow the same approach as demonstrated for the equation of $S_h(t)$. Therefore, it is evident that the assumption of non-uniqueness is false, and the model admits a unique solution given by

$$S_h = S_h^*, \quad I_h = I_h^*, \quad S_g = S_g^*, \quad I_g = I_g^*, \quad S_v = S_v^*, \quad I_v = I_v^*, \quad P = P^*.$$

4. Stability of model in Hyers-Ulam

Definition 4.1. *If there are constants $k_i > 0$ for $i \in \mathbb{N}_1^7$ that fulfill for each σ_i, then the fractal-fractional integrals defined in (3. 7) are considered Hyers-Ulam stable. For $i \in \mathbb{N}_1^7$, the following is true:*

$$\left| S_h(t) - \frac{\beta\,\eta}{\Gamma(\eta)\,KM(\eta)} \int_0^t p^{\beta-1}(t-p)^{1-\eta}\mathbf{C}_1(p, S_h(p))dp + \frac{\beta(1-\eta)\,t^{\beta-1}}{KM(\eta)}\mathbf{C}_1(t, S_h(t)) \right| \leq \sigma_1,$$
$$\left| I_h(t) - \frac{\beta\,\eta}{\Gamma(\eta)\,KM(\eta)} \int_0^t p^{\beta-1}(t-p)^{1-\eta}\mathbf{C}_2(p, I_h(p))dp + \frac{\beta(1-\eta)\,t^{\beta-1}}{KM(\eta)}\mathbf{C}_2(t, I_h(t)) \right| \leq \sigma_2,$$

The rice tungro disease model (2. 2) has an approximate solution, S_h^*, I_h^*, S_g^*, I_g^*, S_v^*, I_v^*, and P^*, that fulfills the model as provided, such that

$$\begin{aligned}
|S_h(t) - S_h^*(t)| &= \left| \frac{\beta\,\eta}{\Gamma(\eta)\,KM(\eta)} \int_0^t p^{\beta-1}(t-p)^{1-\eta}\mathbf{C}_1(p, S_h(p))dp + \frac{\beta(1-\eta)\,t^{\beta-1}}{KM(\eta)}\mathbf{C}_1(t, S_h(t)) - \right. \\
&\quad \left. \left(\frac{\beta\,\eta}{\Gamma(\eta)\,KM(\eta)} \int_0^t p^{\beta-1}(t-p)^{1-\eta}\mathbf{C}_1(p, S_h^*(p))dp + \frac{\beta(1-\eta)\,t^{\beta-1}}{KM(\eta)}\mathbf{C}_1(t, S_h^*(t)) \right) \right|, \\
&= \frac{\beta\,\eta}{\Gamma(\eta)\,KM(\eta)} \int_0^t p^{\beta-1}(t-p)^{1-\eta} |\mathbf{C}_1(p, S_h(p)) - \mathbf{C}_1(p, S_h^*(p))| dp \\
&+ \frac{\beta(1-\eta)\,t^{\beta-1}}{KM(\eta)} |\mathbf{C}_1(t, S_h(t)) - \mathbf{C}_1(t, S_h^*(t))| \\
&\leq \left(\frac{\beta\,\eta}{\Gamma(\eta)\,KM(\eta)} \int_0^t p^{\beta-1}(t-p)^{1-\eta} + \frac{\beta(1-\eta)\,t^{\beta-1}}{KM(\eta)} \right) j_1 \|S_h(t) - S_h^*(t)\| \\
&\quad \times \left[1 - \left(\frac{\eta\,\beta\Gamma(\beta)}{KM(\eta)\,\Gamma(\eta+\beta)} + \frac{\beta(1-\eta)}{KM(\eta)} \right) \right] \|S_h(t) - S_h^*(t)\| \leq 0.
\end{aligned}$$

Letting $\chi_1 = \left[1 - \left(\frac{\eta\,\beta\Gamma(\beta)}{KM(\eta)\,\Gamma(\eta+\beta)} + \frac{\beta(1-\eta)}{KM(\eta)} \right) \right] \|S_h(t) - S_h^*(t)\|$, so the inequality above becomes $|S_h(t) - S_h^*(t)| \leq \chi_1\ j_1$. Similarly for remaining equations of (2. 2), we do like as above equations of $S_h(t)$. And for all remaining equations of model the inequality becomes like as $|I_h(t) - I_h^*(t)| \leq \chi_2\ j_2$, $\left|S_g(t) - S_g^*(t)\right| \leq \chi_3\ j_3$, $\left|I_g(t) - I_g^*(t)\right| \leq \chi_4\ j_4$, $|S_v(t) - S_v^*(t)| \leq \chi_5\ j_5$, $|I_v(t) - I_v^*(t)| \leq \chi_6\ j_6$ and $|P(t) - P^*(t)| \leq \chi_7\ j_7$.

Theorem 4.2. *With assumption , the fractal-fractional rice tungro disease model (2. 2) is HyersUlam stable.*

Proof: Knowing that the fractal-fractional rice tungro disease model (2. 2) has a unique solution. Let there exist an approximate solution of the rice tungro disease model (2. 2), S_h, I_h, S_g, I_g, S_v, I_v, P that satisfies the given model, such that:

$$\begin{aligned}
|S_h(t) - S_h^*(t)| &= \left| \frac{\beta\,\eta}{\Gamma(\eta)\,KM(\eta)} \int_0^t p^{\beta-1}(t-p)^{1-\eta} \mathbf{C}_1(p, S_h(p))dp + \frac{\beta(1-\eta)\,t^{\beta-1}}{KM(\eta)} \mathbf{C}_1(t, S_h(t)) - \right. \\
&\quad \left. \left(\frac{\beta\,\eta}{\Gamma(\eta)\,KM(\eta)} \int_0^t p^{\beta-1}(t-p)^{1-\eta} \mathbf{C}_1(p, S_h^*(p))dp + \frac{\beta(1-\eta)\,t^{\beta-1}}{KM(\eta)} \mathbf{C}_1(t, S_h^*(t)) \right) \right|, \\
&= \frac{\beta\,\eta}{\Gamma(\eta)\,KM(\eta)} \int_0^t p^{\beta-1}(t-p)^{1-\eta} |\mathbf{C}_1(p, S_h(p)) - \mathbf{C}_1(p, S_h^*(p))|dp \\
&+ \frac{\beta(1-\eta)\,t^{\beta-1}}{KM(\eta)} |\mathbf{C}_1(t, S_h(t)) - \mathbf{C}_1(t, S_h^*(t))| \\
&\leq \left(\frac{\beta\,\eta}{\Gamma(\eta)\,KM(\eta)} \int_0^t p^{\beta-1}(t-p)^{1-\eta} + \frac{\beta(1-\eta)\,t^{\beta-1}}{KM(\eta)} \right) j_1 \|S_h(t) - S_h^*(t)\| \\
&\quad \times \left[1 - \left(\frac{\eta\,\beta\Gamma(\beta)}{KM(\eta)\,\Gamma(\eta+\beta)} + \frac{\beta(1-\eta)}{KM(\eta)} \right) \right] \|S_h(t) - S_h^*(t)\| \leq 0.
\end{aligned}$$

Letting $\varpi_1 = \left[1 - \left(\frac{\eta\,\beta\Gamma(\beta)}{KM(\eta)\,\Gamma(\eta+\beta)} + \frac{\beta(1-\eta)}{KM(\eta)} \right) \right] \|S_h(t) - S_h^*(t)\|$, so becomes the above inequality $|S_h(t) - S_h^*(t)| \leq \chi_1\ j_1$ Similarly for remaining equations of (2. 2), we do like as above equations of $S_h(t)$. And for all remaining equations of model the inequality becomes like as $|I_h(t) - I_h^*(t)| \leq \chi_2\ j_2$, $\left|S_g(t) - S_g^*(t)\right| \leq \chi_3\ j_3$, $\left|I_g(t) - I_g^*(t)\right| \leq \chi_4\ j_4$, $|S_v(t) - S_v^*(t)| \leq \chi_5\ j_5$, $|I_v(t) - I_v^*(t)| \leq \chi_6\ j_6$ and $|P(t) - P^*(t)| \leq \chi_7\ j_7$. Consequently, the fractal-fractional model of rice tungro illness (2. 2) is by definition Hyers-Ulam stable. The evidence is finished now.

5. Model's Reproductive Number and Equilibrium Point

The point of equilibrium in this model that is free of sickness with absence predators:

$$E_0 = \left\{ S_h = \frac{\phi_h}{\alpha_h}, I_h = 0, S_g = \frac{\phi_g}{\alpha_g}, I_g = 0, S_v = \frac{\phi_v}{\alpha_v + \delta_v}, I_v = 0, P = 0 \right\},$$

The point of equilibrium in this model that is free of sickness:

$$E_1 = \left\{ S_h = \frac{\phi_h}{\alpha_h}, I_h = 0, S_g = \frac{\phi_g}{\alpha_g}, I_g = 0, S_v = \frac{\phi_v}{\alpha_v + \delta_v}, I_v = 0, P = \frac{\delta_v \phi_v}{\gamma_1\,(\alpha_v + \delta_v)} \right\},$$

as well as endemic points are $E^* = (S_h^*, I_h^*, S_g^*, I_g^*, S_v^*, I_v^*, P^*)$ where

$$\begin{aligned}
S_h^* &= \frac{(\alpha_v+\delta_v)\left((d_h+\alpha_h)(\alpha_v+\delta_v)+\beta_3\phi_h\right)}{\beta_3\left(\alpha_h(\alpha_v+\delta_v)+\beta_1\phi_v\right)}; \quad I_h^* = \frac{\beta_1\beta_3\phi_h\phi_v - \alpha_h(d_h+\alpha_h)(\alpha_v+\delta_v)^2}{\beta_3(d_h+\alpha_h)\left(\alpha_h(\alpha_v+\delta_v)+\beta_1\phi_v\right)};\\
S_g^* &= \frac{\beta_1\phi_g(\alpha_v+\delta_v)\left((d_h+\alpha_h)(\alpha_v+\delta_v)+\beta_3\phi_h\right)}{d_h(\alpha_v+\delta_v)^2(\beta_1\alpha_g-\beta_2\alpha_h)+(\alpha_v+\delta_v)X_1+\beta_1\beta_2\beta_3\phi_h\phi_v};\\
I_g^* &= -\frac{\beta_2\phi_g\left(\alpha_h(d_h+\alpha_h)(\alpha_v+\delta_v)^2-\beta_1\beta_3\phi_h\phi_v\right)}{(d_g+\alpha_g)\left(d_h(\alpha_v+\delta_v)^2(\beta_1\alpha_g-\beta_2\alpha_h)+(\alpha_v+\delta_v)X_1+\beta_1\beta_2\beta_3\phi_h\phi_v\right)};\\
S_v^* &= \frac{(d_h+\alpha_h)\left(\alpha_h(\alpha_v+\delta_v)+\beta_1\phi_v\right)}{\beta_1\left((d_h+\alpha_h)(\alpha_v+\delta_v)+\beta_3\phi_h\right)}; \qquad I_v^* = \frac{\beta_1\beta_3\phi_h\phi_v-\alpha_h(d_h+\alpha_h)(\alpha_v+\delta_v)^2}{\beta_1(\alpha_v+\delta_v)\left((d_h+\alpha_h)(\alpha_v+\delta_v)+\beta_3\phi_h\right)};\\
P^* &= \frac{\delta_v\phi_v}{\gamma_1(\alpha_v+\delta_v)},
\end{aligned}$$

where $X_1 = \left(\beta_1\beta_3\alpha_g\phi_h + \alpha_h(\alpha_v+\delta_v)(\beta_1\alpha_g-\beta_2\alpha_h)\right)$. If the equilibrium point of the proposed model is asymptotically stable for all delay values, the model is considered absolutely stable; otherwise, it is conditionally stable for certain delay intervals but not for all. The basic reproduction number is given by

$$R_0 = \frac{\sqrt{\beta_1}\sqrt{\beta_3}\sqrt{\phi_h}\sqrt{\phi_v}}{\sqrt{\alpha_h}\sqrt{d_h+\alpha_h}(\alpha_v+\delta_v)}.$$

6. Analysis of Bifurcation

In this section, we use bifurcation theory to analyze the bifurcation occurring at the equilibrium point E_1.

Analysis of the bifurcation at the equilibrium point E_1 in the rice tungro virus model

The eigenvalue computation shows that none of the eigenvalues equals ± 1, which suggests the possibility of a flip bifurcation in the system. The parameter set is denoted by

$$(\phi_h,\ \phi_g,\ \phi_v,\ \beta_1,\ \alpha_h,\ \beta_2,\ \alpha_g,\ \alpha_v,\ \delta_v).$$

$$F|E_1 = \left\{(\phi_h,\phi_g,\phi_v,\beta_1,\alpha_h,\beta_2,\alpha_g,\alpha_v,\delta_v) : \alpha_g = \frac{d_h}{2}, \alpha_g = \frac{d_g}{2}, \alpha_v = \frac{\delta_v}{2},\right\}. \quad (6.\ 9)$$

The following theorem states that for system (2. 2), there exists no flip-type bifurcation at

$$(\phi_h,\ \phi_g,\ \phi_v,\ \beta_1,\ \alpha_h,\ \beta_2,\ \alpha_g,\ \alpha_v,\ \delta_v) \in F(E_1).$$

Theorem 6.1. *Given the model* (2. 2) *with parameters*

$$(\phi_h,\ \phi_g,\ \phi_v,\ \beta_1,\ \alpha_h,\ \beta_2,\ \alpha_g,\ \alpha_v,\ \delta_v) \in F(E_1),$$

the system does not exhibit a flip bifurcation.

Proof:

By restricting the study of model (2. 2) to the subspace where $I_h = I_g = I_v = P = 0$, we can analyze the bifurcation behavior. This restriction is valid because model (2. 2) is

invariant under the conditions $I_h = I_g = I_v = P = 0$, resulting in the following reduced form:

$$S_h^{t+1} = \phi_1 - \alpha_h S_h; \quad S_g^{t+1} = \phi_2 - \alpha_g S_g; \quad S_v^{t+1} = \phi_3 - (\alpha_v + \delta_v) S_v. \quad (6.\ 10)$$

From 6. 10 , one denotes map

$$f_1(S_h) = \phi_1 - \alpha_h S_h; \quad f_2(S_g) = \phi_2 - \alpha_g S_g; \quad f_3(S_v) = \phi_3 - (\alpha_v + \delta_v) S_v. \quad (6.\ 11)$$

Now if $\alpha_g = \frac{d_h}{2}, \alpha_g = \frac{d_g}{2}, \alpha_v = \frac{\delta_v}{2}$ and $S_h = S_h^* = \frac{\phi_1}{\alpha_h}$, $S_g = S_g^* = \frac{\phi_2}{\alpha_g}$, $S_v = S_v^* = \frac{\phi_2}{\alpha_v + \delta_v}$ then from 6. 11 we get

$$\frac{\partial f_1}{\partial S_h} = -\alpha_h = -\frac{d_h}{2} \neq 0; \quad \frac{\partial f_2}{\partial S_g} = -\alpha_v = -\frac{d_h}{2} \neq 0; \quad \frac{\partial f_3}{\partial S_v} = -(\alpha_v + \delta_v) = -\frac{3\delta_v}{2} \neq 0,$$
$$\frac{\partial f_1}{\partial \alpha_h} = S_h = -S_h^* \neq 0; \quad \frac{\partial f_2}{\partial \alpha_g} = S_g = -S_g^* \neq 0; \quad \frac{\partial f_3}{\partial \alpha_v} = S_v = -S_v^* \neq 0,$$

and

$$\frac{\partial^2 f_1}{\partial S_h^2} = 0; \quad \frac{\partial^2 f_2}{\partial S_g^2} = 0; \quad \frac{\partial^2 f_3}{\partial S_v^2} = 0. \quad (6.\ 12)$$

The computations above indicate that there is no flip bifurcation for model (2. 2) at the equilibrium point E_1, since the parametric condition (6. 12) fails to satisfy the non-degeneracy requirement for

$$(\phi_h,\ \phi_g,\ \phi_v,\ \beta_1,\ \alpha_h,\ \beta_2,\ \alpha_g,\ \alpha_v,\ \delta_v) \in F(E_1).$$

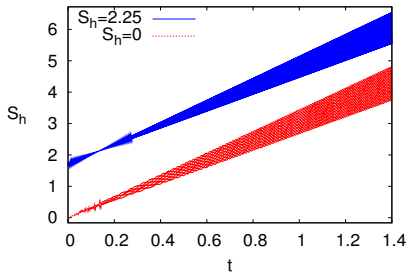

(A) S_h under parameter ϕ_h

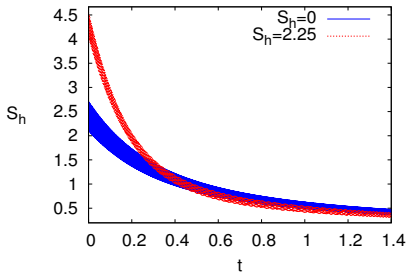

(B) S_h under parameter β_1

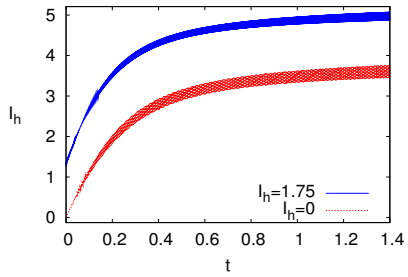

(C) I_h under parameter β_1

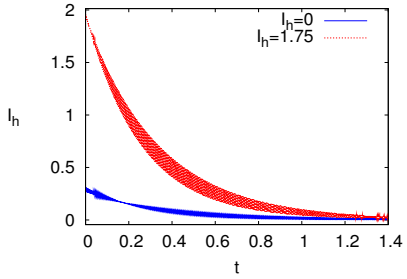

(D) I_h under parameter α_h

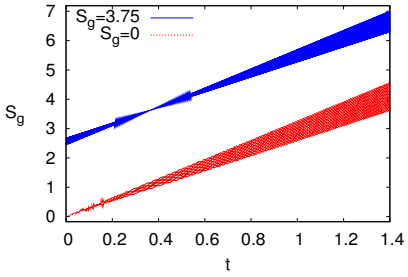

(E) S_g under parameter ϕ_g

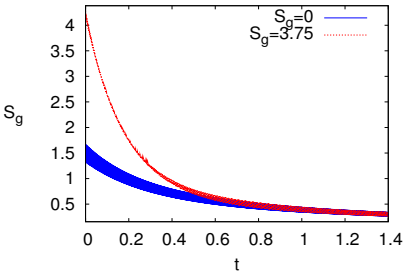

(F) S_g under parameter β_2

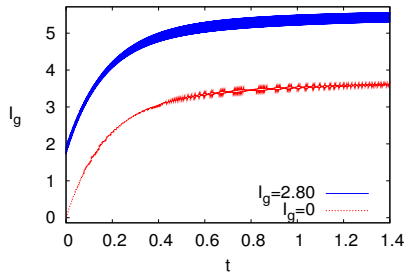

(G) I_g under parameter β_2

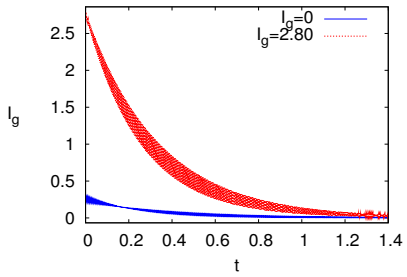

(H) I_g under parameter α_g

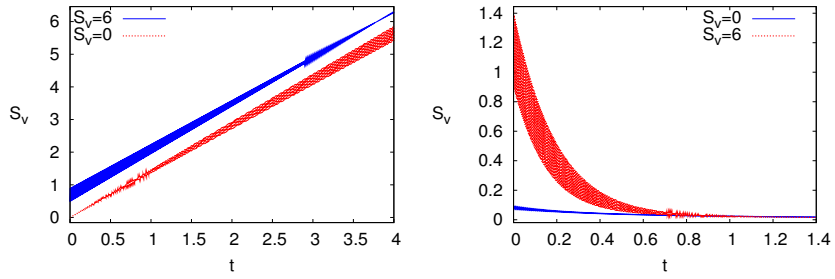

(I) S_v under parameter ϕ_v (J) S_v under parameter β_3

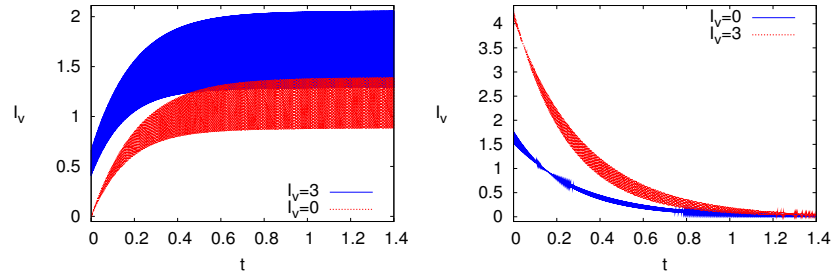

(K) I_v under parameter β_3 (L) I_v under parameter δ_v

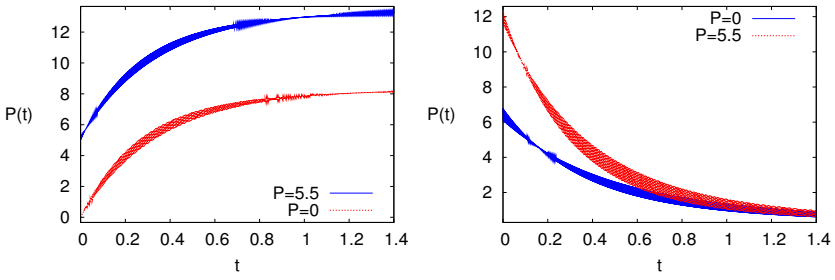

(M) $P(t)$ under parameter δ_V (N) $P(t)$ under parameter γ_1

FIGURE 2. Bifurcation Graphs

The newly designed model under investigation analyzes various infectious measures of rice tungro disease. The model's impacts on trees are quite complex, and it describes a continuous time-dependent system. According to the hypotheses of the model, several parameters are used, including: $\phi_h = 0.75$, $\beta_1 = 0.02$, $\alpha_h = 0.05$, $d_h = 0.031$, $\phi_g = 0.5$, $\beta_2 = 0.01$, $\alpha_g = 0.091$, $d_g = 0.031$, $\phi_v = 0.05$, $\beta_3 = 0.076$, $\alpha_v = 0.057$, $\delta_v = 0.43$

and $\gamma_1 = 0.021$. The linearization technique is employed in Figure (2) to demonstrate the stability and boundedness of the model's equations. The linearization technique is used in Figure (2) to accomplish the stability and boundedness of the equation model. In this case, we have constructed the bifurcation diagram of the continuous time graph of the model about different parametric values in certain ranges, like β_1, 0 to 1. We can ascertain the continuous model's stable condition by including the rice tungro disease and different measures. Our theoretical results are supported by time-steady graphs in Figure (2), which show the rate of parametric values of the total requirement rate.

7. Solutions by Fractal Fractional Operator

Now, we will apply the numerical method to solve our newly generated model, denoted by equation 2. 2 . In this instance, we replace the classical derivative operator with the ML kernel. The version with a flexible order will also be used. We also consider the model in its variable-order form. For clarity, equation (2. 2) can be expressed as follows:

$$\begin{aligned}
{}_0^{FFM}D_t^{\eta,\beta}S_h &= \phi_h - \beta_1 S_h I_v - \alpha_h S_h;\\
{}_0^{FFM}D_t^{\eta,\beta}I_h &= \beta_1 S_h I_v - (\alpha_h + d_h) I_h;\\
{}_0^{FFM}D_t^{\eta,\beta}S_g &= \phi_g - \beta_2 S_g I_v - \alpha_g S_g;\\
{}_0^{FFM}D_t^{\eta,\beta}I_g &= \beta_2 S_g I_v - (\alpha_g + d_g) I_g;\\
{}_0^{FFM}D_t^{\eta,\beta}S_v &= \phi_v - \beta_3 S_v I_h - (\alpha_v + \delta_v) S_v;\\
{}_0^{FFM}D_t^{\eta,\beta}I_v &= \beta_3 S_v I_h - (\alpha_v + \delta_v) I_v;\\
{}_0^{FFM}D_t^{\eta,\beta}P &= \delta_v (S_v + I_v) - \gamma_1 P.
\end{aligned}$$

After applying the Mittag-Leffler kernel and the fractal-fractional integral, we obtain the following results.

$$\begin{aligned}
S_h(t_{k+1}) &= S_{h0} + \frac{1-\eta}{KM(\eta)} t_k^{1-\beta} S_{h1}(t_k, S_h(t_k), I_h(t_k), S_g(t_k), I_g(t_k), S_v(t_k), I_v(t_k), P(t_k))\\
&+ \hbar \sum_{w=2}^{k} \int_{t_w}^{t_{w+1}} S_{h1}(t,\pi)\beta^{1-\beta}(t_{k+1}-\beta)^{1-\eta} d\beta.
\end{aligned}$$

Where $\pi = S_h, I_h, S_g, I_g, S_v, I_v, P$ and $\hbar = \frac{\eta}{KM(\eta)\Gamma(\eta)}$. Here, we recall the Newton polynomial. After substituting the Newton polynomial into the preceding equations, the integrals in those equations can be evaluated using the corresponding numerical methods. Consequently, we obtain the following final expressions:

$$
\begin{aligned}
S_{h(k+1)} &= S_{h0} + \frac{1-\eta}{KM(\eta)} t_k^{1-\beta} S_{h1}(t_k, S_h(t_k), I_h(t_k), S_g(t_k), I_g(t_k), S_v(t_k), I_v(t_k), P(t_k)) \\
&+ \hbar \sum_{w=2}^{k} S_{h1}[t_{w-2}, S_h^{w-2}, I_h^{w-2}, S_g^{w-2}, I_g^{w-2}, S_v^{w-2}, I_v^{w-2}, P^{w-2}] t_{w-2}^{1-\beta} \\
&\times \frac{(\triangle t)^{\eta}}{\eta} \left[(k-w+1)^{\eta} - (k-w)^{\eta}\right] + \hbar \sum_{w=2}^{k} \frac{1}{\triangle t} \Big\{ t_{w-1}^{1-\beta} S_{h1}(t_{w-1}, S_h^{w-1}, I_h^{w-1}, S_g^{w-1}, I_g^{w-1}, \\
&\quad S_v^{w-1}, I_v^{w-1}, P^{w-1}) - t_{w-2}^{1-\beta} S_{h1}[t_{w-2}, S_h^{w-2}, I_h^{w-2}, S_g^{w-2}, I_g^{w-2}, S_v^{w-2}, I_v^{w-2}, P^{w-2}] \Big\} \\
&\times \frac{(\triangle t)^{\eta+1}}{\eta(\eta+1)} \left[(k-w+1)^{\eta}(k-w+3+2\eta) - (k-w)^{\eta}(k-w+3+3\eta)\right] \\
&+ \hbar \sum_{w=2}^{k} \frac{1}{2\triangle t^2} \Big\{ t_i^{1-\beta} S_{h1}[t_w, S_h^{w}, I_h^{w}, S_g^{w}, I_g^{w}, S_v^{w}, I_v^{w}, P^{w}] \\
&\quad -2t_{w-1}^{1-\beta} S_{h1}(t_{w-1}, S_h^{w-1}, I_h^{w-1}, S_g^{w-1}, I_g^{w-1}, S_v^{w-1}, I_v^{w-1}, P^{w-1}) + t_{w-2}^{1-\beta} S_{h1} \\
&\quad [t_{w-2}, S_h^{w-2}, I_h^{w-2}, S_g^{w-2}, I_g^{w-2}, S_v^{w-2}, I_v^{w-2}, P^{w-2}] \Big\} \times \frac{(\triangle t)^{\eta+2}}{\eta(\eta+1)(\eta+2)} \\
&\quad \Bigg[(k-w+1)^{\eta} \Big\{ 2(k-w)^2 + (3\eta+10)(k-w) + 2\eta^2 + 9\eta + 12 \Big\} - \\
&\quad (k-w)^{\eta} \Big\{ 2(k-w)^2 + (5\eta+10)(k-w) + 6\eta^2 + 18\eta + 12 \Big\} \Bigg]
\end{aligned}
$$

Similarly, for the remaining equations in (2. 2), we proceed as demonstrated for the equation of $S_h(t)$. This completes the numerical scheme for model (2. 2) in the sense of the fractal-fractional derivative with the Mittag-Leffler kernel.

7.1. Advantages and Disadvantages of the Fractional-Order Model. Advantages

- **Captures Memory and Delayed Effects:** Fractional-order derivatives model memory effects and delayed responses in dynamic systems, which are often present in real-world processes like climate change, disease spread, and ecological systems.
- **Improved Accuracy:** The fractional-order approach provides a more accurate representation of complex phenomena that exhibit non-local and non-linear behaviors, which integer-order models cannot capture.
- **Greater Flexibility:** It offers flexibility in modeling systems with a variety of dynamics, allowing for more realistic simulations in various fields such as biology, physics, and engineering.
- **Better Fit for Real-World Systems:** For long range duration and memory effect fractional derivative is good and also clear with natural system.

Disadvantages

- **More Complexity in Computation:** Higher computing costs and more intricate numerical techniques are frequently the results of include fractional derivatives.

- **Hard Parameter Requirement:** The estimation of parameters of fractional model is so difficult by comparing with integer order model.
- **The Challenges of Interpretation:** In certain situations, it might be more difficult to intuitively comprehend the behavior of the model due to the more abstract nature of the physical interpretation of fractional-order derivatives.
- **Limited Software and Tools:** For use of clear calculation, fractional derivatives used some special type softwares which are not easily available.

8. Simulation Explanation

8.1. **Analysis and Simulation of Parameter Effects in 3D.** In Fig. 3, the impact of β_1 rate of transfer from susceptible to infected healthy plants class due to infected vectors on all compartments of fractional rice model, which shoes the threshold shedding throughout time. Consequently, β_1 is essential for assessing the level of infection healthy in the rice population.

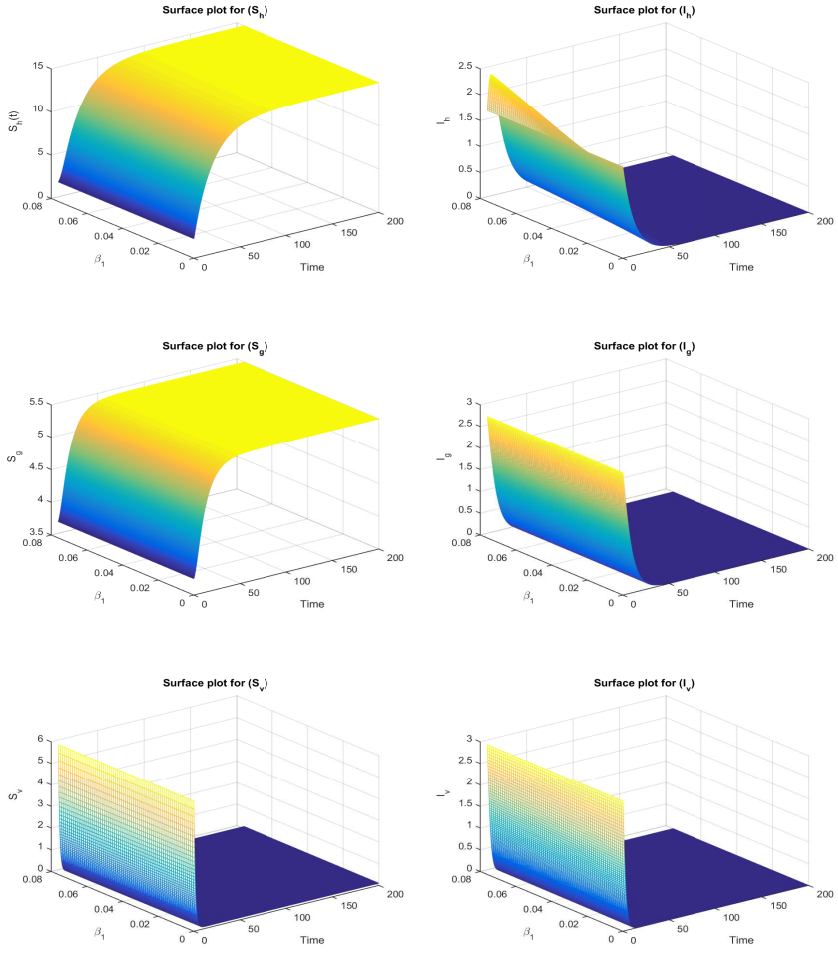

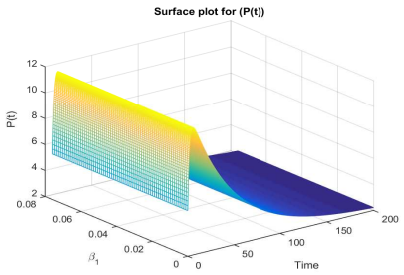

FIGURE 3. Simulation of all compartment of the system for β_1.

In Fig. 4, the impact of β_2 rate of transfer from susceptible to infected growing plants class due to infected vectors on all compartments of fractional rice model, which shoes the threshold shedding throughout time. Consequently, β_2 is essential for assessing the level of infection growing in the rice population.

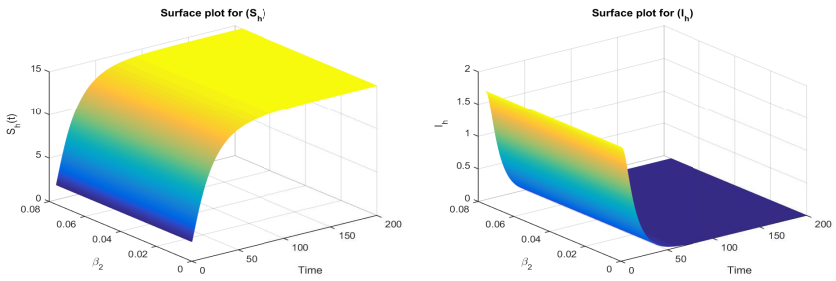

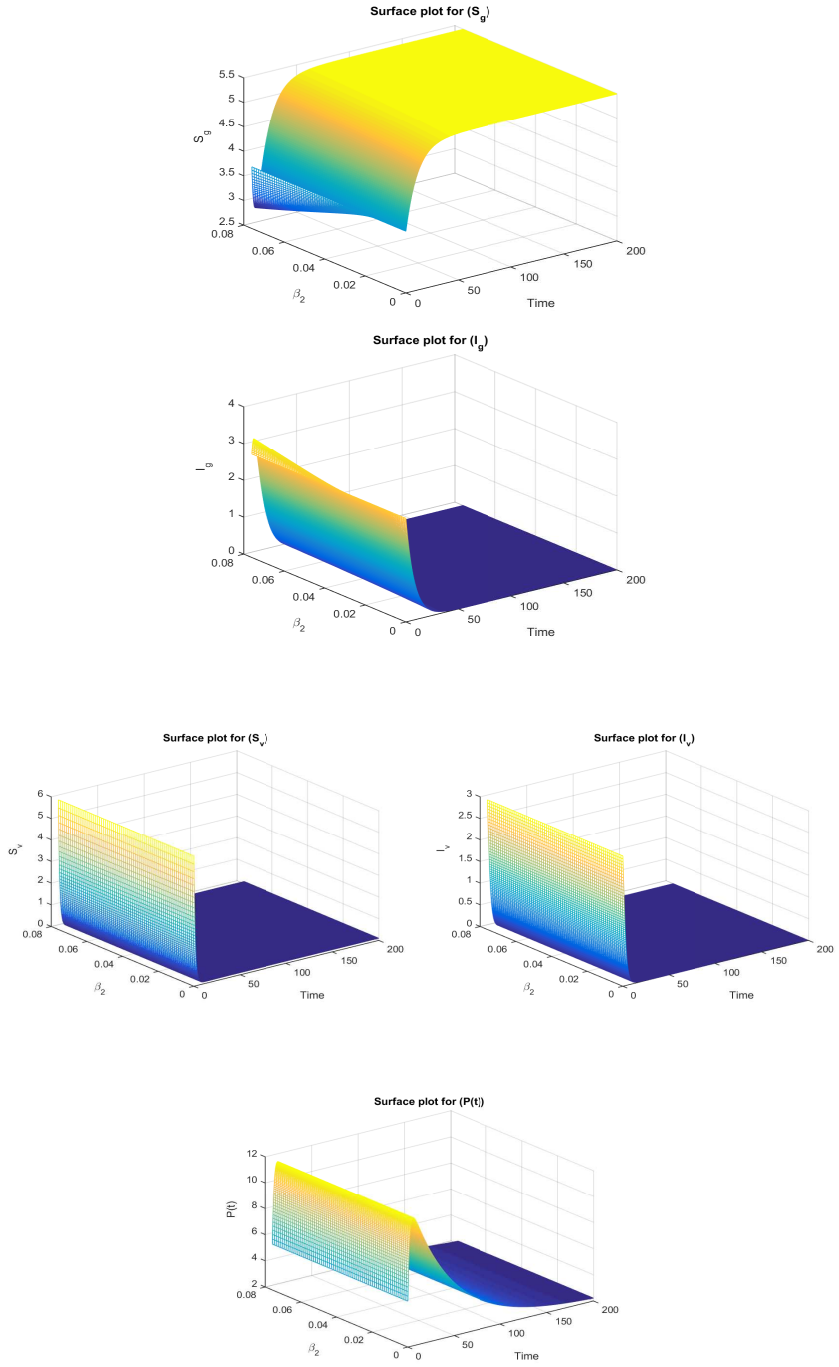

FIGURE 4. Simulation of all compartment of the system for β_2.

In Fig. 5, the impact of β_3 rate of transfer from susceptible to infected vector class due to infected healthy plants on all compartments of fractional rice model, which shoes the threshold shedding throughout time. Consequently, β_3 is essential for assessing the level of infection vectors in the rice population.

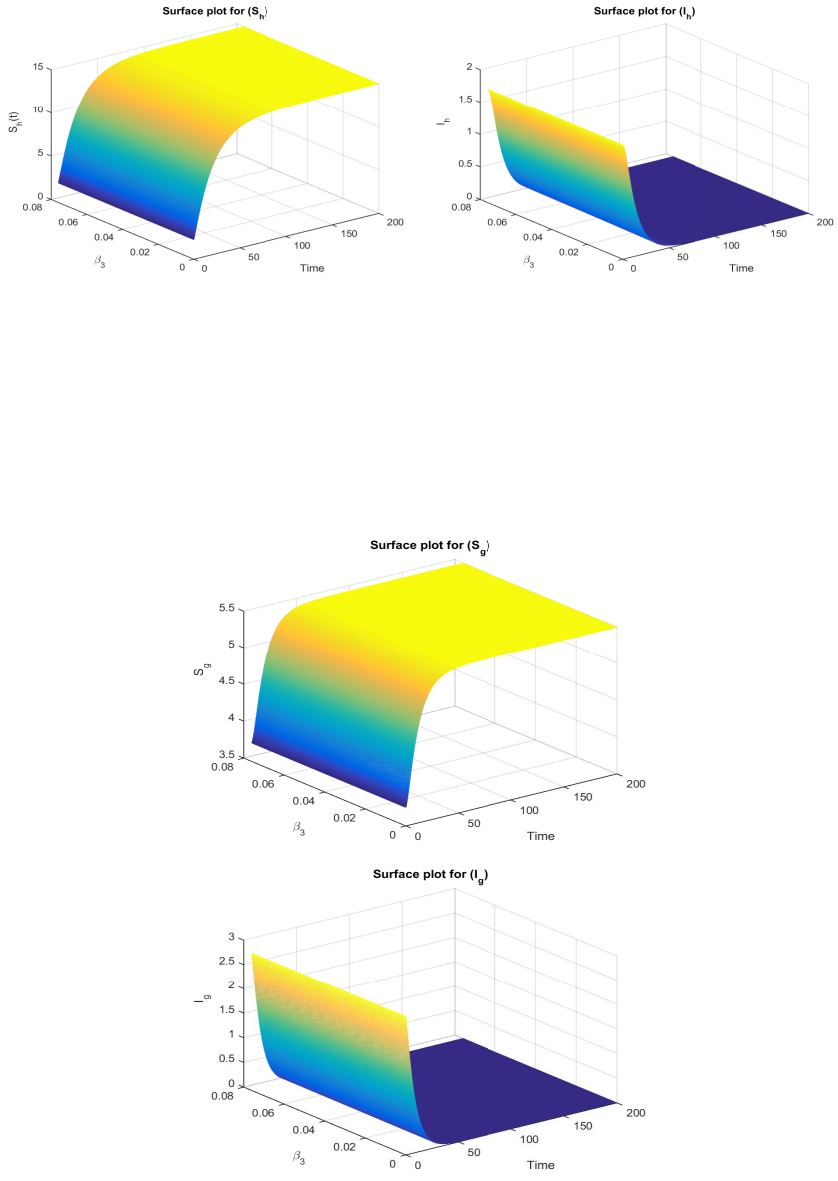

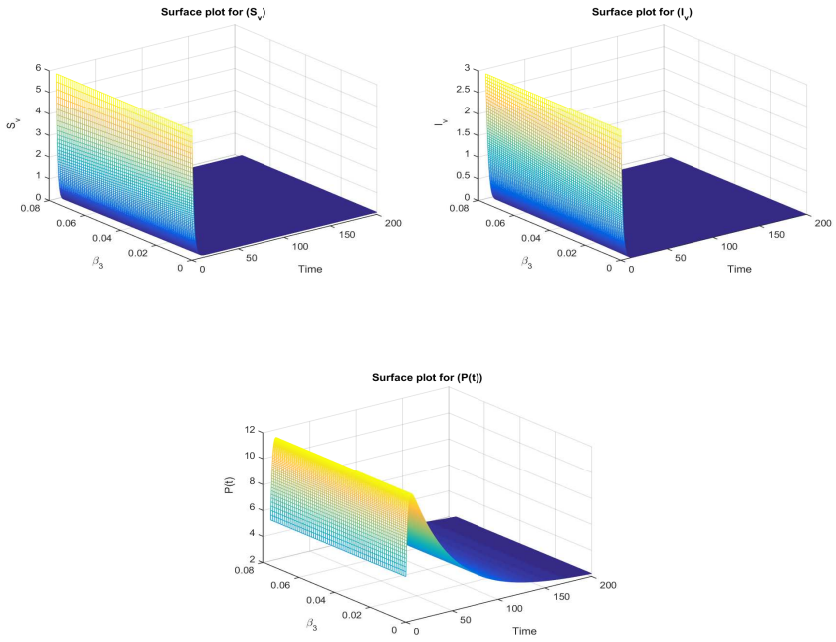

FIGURE 5. Simulation of all compartment of the system for β_3.

In particular, we now emphasize how tactics for limiting viral propagation in agricultural systems like rice may be informed by adjustments to the model's parameters, such as the shedding rates β_1, β_2, and β_3. We also discuss the potential for applying our findings to improve early detection, optimize interventions, and reduce infection rates by controlling factors such as virus shedding and transmission. This enhances the relevance of our model and its implications for practical disease management.

8.2. **Simulation of the Fractal-Fractional Model (FFM).** The effectiveness of the derived theoretical results is demonstrated through the following simulations. The mathematical analysis of the rice tungro disease yields insightful outcomes when fractional (non-integer) order parameters are employed. As the fractional orders decrease, the solutions for S_h, I_h, S_g, I_g, S_v, I_v, and P shown in Figures 6–12 approach their expected steady-state values. The numerical simulations of the fractional-order rice tungro disease model were implemented using MATLAB. The initial conditions for the system are set as $S_h(0) = 2.25$, $I_h(0) = 1.75$, $S_g(0) = 3.75$, $I_g(0) = 2.80$, $S_v(0) = 6$, $I_v(0) = 3$, and $P(0) = 5.5$ for the respective sub-compartments. The parameter values used are: $\phi_h = 0.75$, $\beta_1 = 0.02$, $\alpha_h = 0.05$, $d_h = 0.031$, $\phi_g = 0.5$, $\beta_2 = 0.01$, $\alpha_g = 0.091$, $d_g = 0.031$, $\phi_v = 0.05$, $\beta_3 = 0.076$, $\alpha_v = 0.057$, $\delta_v = 0.43$, $\gamma_1 = 0.021$.

Figures 6–12 illustrate the graphical behavior of the rice tungro disease model based on the proposed numerical method, comparing fractional-order results with classical integer-order solutions. The dynamics of susceptible healthy plants S_h and susceptible growing plants S_g are presented in Figures 6 and 8, respectively. In these cases, all compartments

exhibit a rising trend, eventually stabilizing due to an increase in the recovered population. The infected healthy plants I_h, infected growing plants I_g, susceptible vectors S_v, and infected vectors I_v are depicted in Figures 7, 9, 10, and 11, respectively. These compartments show a steady decline over time, approaching equilibrium as recovery increases. Furthermore, the predator populations, both with and without medication, increase as the fractional orders decrease, as shown in Figure 12. Figures 6a–12a and 6b–12b compare the system behavior for fractional orders 0.6 and 0.4, respectively. While the overall dynamics are similar for both fractional orders, lower fractional values tend to produce more accurate and stable results. This analysis highlights future research directions aimed at reducing the number of diseased plants and infected vectors in the environment. For all sub-compartments, the Caputo fractional derivative provides better modeling accuracy than classical derivatives. Additionally, the solutions become more precise and reliable as the fractional orders decrease.

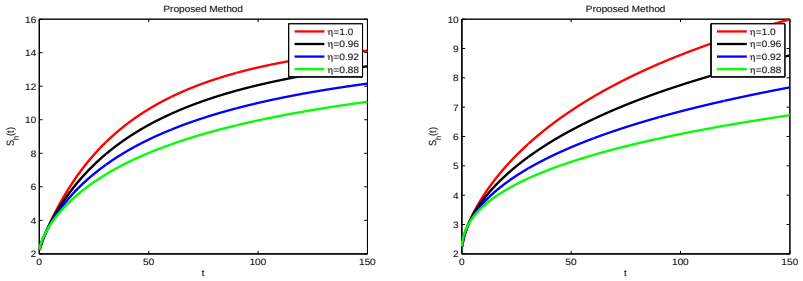

(A) $\beta = 0.8$ (B) $\beta = 0.6$

FIGURE 6. Simulation of $S_h(t)$ for different fractal dimensions β and fractional orders η.

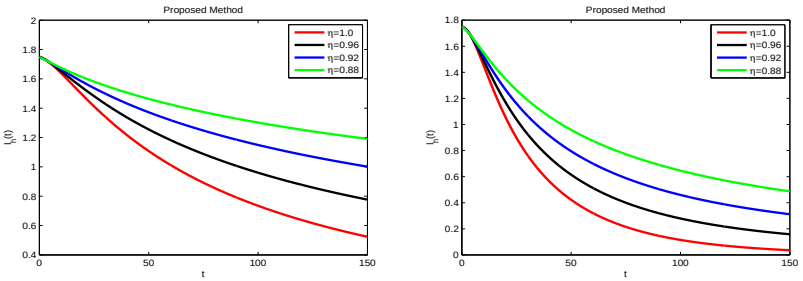

(A) $\beta = 0.8$ (B) $\beta = 0.6$

FIGURE 7. Simulation of $I_h(t)$ for different fractal dimensions β and fractional orders η.

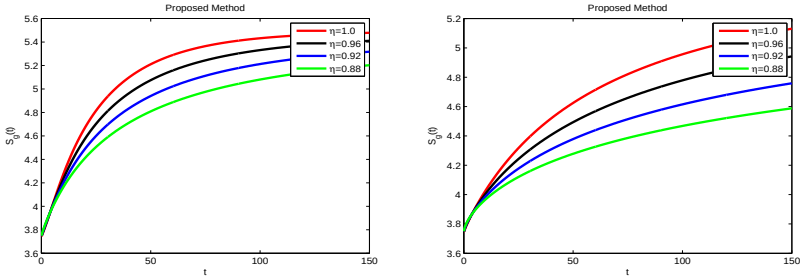

(A) $\beta = 0.8$ (B) $\beta = 0.6$

FIGURE 8. Simulation of $S_g(t)$ for different fractal dimensions β and fractional orders η.

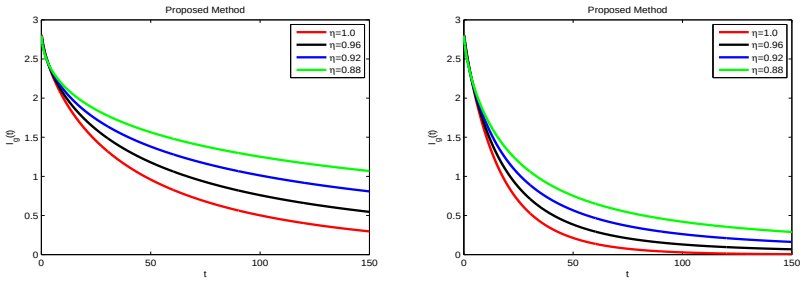

(A) $\beta = 0.8$ (B) $\beta = 0.6$

FIGURE 9. Simulation of $I_g(t)$ for different fractal dimensions β and fractional orders η.

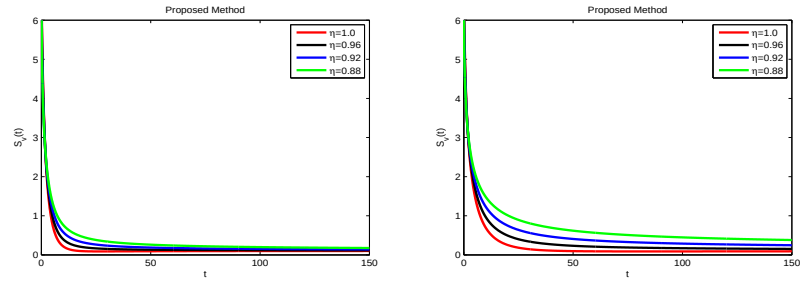

(A) $\beta = 0.8$ (B) $\beta = 0.6$

FIGURE 10. Simulation of $S_v(t)$ for different fractal dimensions β and fractional orders η.

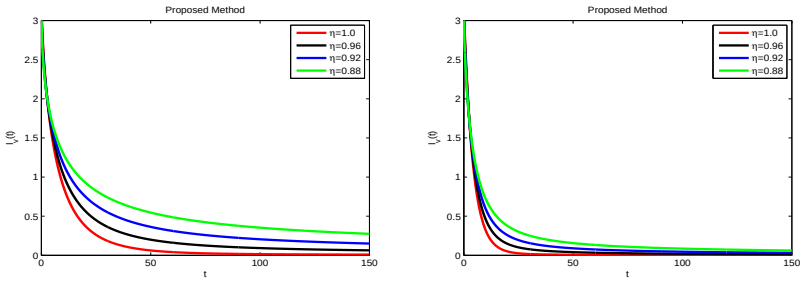

(A) $\beta = 0.8$ (B) $\beta = 0.6$

FIGURE 11. Simulation of $S_v(t)$ for different fractal dimensions β and fractional orders η.

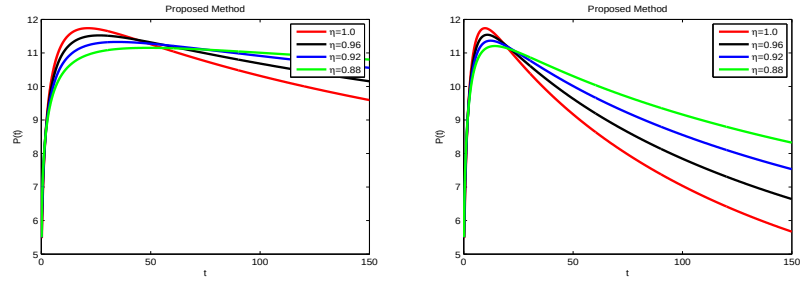

(A) $\beta = 0.8$ (B) $\beta = 0.6$

FIGURE 12. Simulation of $P(t)$ for different fractal dimensions β and fractional orders η.

9. CONCLUSION

This work develops a fractional-order model for rice tungro disease without pharmacological treatment, utilizing the Fractal-Fractional Operator (FFO) to generate reliable data. The model provides guidelines for early disease detection and removal by introducing control measures, such as cutting and burying infected plants, to prevent the diseases spread. We analyze the diseases impact across different infectious stages and verify the systems stability both qualitatively and numerically, confirming the existence of bounded and unique solutions. Our study evaluates global efforts to control rice tungro and examines how infection rates change following asymptomatic interventions. Using the FFO, we continuously track disease progression in plants and their surroundings. Numerical simulations employing a two-step Lagrange polynomial method illustrate how various factors influence the disease dynamics and highlight the role of the fractional operator in capturing complex, nonlocal interactions. The model incorporates hypersensitive response (HR)

mechanisms that enhance plant resistance against bacterial infection. This approach advances understanding of rice tungro by improving long-term forecasts and revealing intricate disease behaviors under different fractional orders. Ultimately, this analysis supports effective management and control strategies, contributing valuable insights for future research aimed at reducing the diseases environmental and agricultural impact.

DATA AVAILABILITY

No data.

CONFLICT OF INTEREST

The authors declare that there is no conflict of interest regarding the publication of this paper.

FUNDING

The authors did not receive any specific funding for this work.

REFERENCES

[1] M. E. Abo, and H. A. Fadhil. Epidemiology and management of rice viruses and virus diseases. *Plant Virology in Sub-Saharan Africa*, IITA (2003): 112.

[2] A. Ahmad, K. Faiz, M. Farman, S. Sattar, and A. Sambas. Control and effect of climate change due to human activities by mathematical modeling approach under fractional operator. *Model. Earth Syst. Environ.*, 11, No. 4 (2025): 121.

[3] A. Ahmad, M. Farman, P. A. Naik, K. Faiz, A. Ghaffar, E. Hincal, and M. U. Saleem. Analytical analysis and bifurcation of pine wilt dynamical transmission with host vector and nonlinear incidence using sustainable fractional approach. *Partial Diff. Eq. Appl. Math.*, 11 (2024): 100830.

[4] A. Atangana. Modelling the spread of COVID-19 with new fractal-fractional operators: can the lockdown save mankind before vaccination? *Chaos Solitons Fractals*, 136 (2020): 109860.

[5] N. Aziz, S. T. Rizvi, K. Ali, and A. R. Seadawy. Bifurcation and sensitivity analysis along with the numerical simulations of susceptible breaking-out quarantine treatment recovered computer model. *Int. J. Model. Simul. Sci. Comput.*, 15, No. 6 (2024).

[6] N. J. Cunniffe, B. Koskella, C. J. E. Metcalf, S. Parnell, T. R. Gottwald, and C. A. Gilligan. Thirteen challenges in modelling plant diseases. *Epidemics*, 10, No. 1 (2015): 610.

[7] A. Devaux, J. P. Goffart, A. Petsakos, P. Kromann, M. Gatto, J. Okello, and G. Hareau. Global food security, contributions from sustainable potato agri-food systems. In: *The Potato Crop*, Springer (2020): 335.

[8] A. Ghaffar, K. Faiz, and A. Ahmad. Investigation and bifurcation analysis of the ocean system impact on climate change utilizing mathematical modeling approach. *Model. Earth Syst. Environ.*, 11, No. 3 (2025): 122.

[9] J. Guckenheimer, and P. Holmes. *Nonlinear oscillations, dynamical systems, and bifurcations of vector fields*. Vol. 42, Springer (2013).

[10] D. D. Headey. The impact of the global food crisis on self-assessed food security. *World Bank Econ. Rev.*, 27, No. 1 (2013): 127.

[11] U. IFAD. The state of food security and nutrition in the world 2017. *FAO* (2017).

[12] J. W. Jones, J. M. Antle, B. Basso, K. J. Boote, R. T. Conant, I. Foster, and T. R. Wheeler. Brief history of agricultural systems modeling. *Agric. Syst.*, 155 (2017): 240254.

[13] S. Khan, K. Shah, A. Debbouche, S. Zeb, and V. Antonov. Solvability and Ulam-Hyers stability analysis for nonlinear piecewise fractional cancer dynamic systems. *Phys. Scr.*, 99, No. 2 (2024): 025225.

[14] Y. A. Kuznetsov. Numerical analysis of bifurcations. In: *Elements of Applied Bifurcation Theory*, Springer (2004): 505585.

[15] P. S. Rao, and A. Hasanuddin. Incidence of rice tungro virus disease and its vector in South Sulawesi, Indonesia. *Int. J. Pest Manag.*, 37, No. 3 (1991): 256258.

[16] A. Raza, K. Ali, S. T. Rizvi, S. Sattar, and A. R. Seadawy. Discussion on vector control dengue epidemic model for stability analysis and numerical simulations. *Braz. J. Phys.*, 55, No. 1 (2025): 21.

[17] S. T. Rizvi, A. R. Seadawy, S. K. Naqvi, and M. Ismail. Bifurcation analysis for mixed derivative nonlinear Schrdingers equation, α-helix nonlinear Schrdingers equation and Zoomeron model. *Opt. Quantum Electron.*, 56, No. 3 (2024): 452.

[18] W. Suryaningrat, N. Anggriani, A. K. Supriatna, and N. Istifadah. The optimal control of rice tungro disease with insecticide and biological agent. *AIP Conf. Proc.*, 2264, No. 1 (2020): 060014.

[19] W.-B. Zhang. *Discrete dynamical systems, bifurcations and chaos in economics*. Elsevier (2006).